J|A|C|S
ARTICLES
Published on Web 01/04/2007

From Insulator to Electride: A Theoretical Model of Nanoporous Oxide $12CaO \cdot 7Al_2O_3$

Peter V. Sushko,*,† Alexander L. Shluger,† Masahiro Hirano,‡ and Hideo Hosono§

Contribution from the Department of Physics & Astronomy, University College London, Gower Street, London WC1E 6BT, U.K., SORST, Japan Science and Technology Agency, P.O. Box S2-13, Tokyo Institute of Technology, 4259 Nagasuta, Midori-ku, Yokohama 226-8503, Japan, and Frontier Collaborative Research Center and Materials and Structures Laboratory, Tokyo Institute of Technology, 4259 Nagasuta, Midori-ku, Yokohama 226-8503, Japan

Received September 1, 2006; E-mail: p.sushko@ucl.ac.uk

Abstract: Recently, a novel inorganic electride stable at room temperatures has been obtained by reducing a complex nanoporous oxide $12CaO \cdot 7Al_2O_3$ (C12A7) in a Ca atmosphere (Matsuishi, S.; Toda, Y.; Miyakawa, M.; Hayashi, K.; Kamiya, T.; Hirano, M.; Tanaka, I.; Hosono, H. *Science* **2003**, *301*, 626). In this system, up to $2.3 \times 10^{21}/cm^3$ electrons can be accommodated in a three-dimensional network of cages formed by a positively charged oxide framework. We demonstrate theoretically that at all concentrations, n_e, the electrons are neither associated with specific atoms nor fully delocalized. At low n_e, the electrons are isolated from each other and resemble the color centers in insulating materials. They are well localized in some of the lattice cages and yield strong inhomogeneous lattice distortions that provide polaron-type cage-to-cage electron hopping. As n_e increases, the electrons form a denser electron gas and become more evenly spread over all available lattice cages. At sufficiently high n_e, the system becomes metallic but still retains partially localized character of the conducting electrons. We describe the nature of the electronic states at the Fermi level and predict the changes in the optical and magnetic properties of this system as a function of n_e.

1. Introduction

Electrides are crystalline ionic materials in which electrons serve as anions.[1,2] Tremendous effort has been made to develop electrides that would be robust enough to be used in practical applications at ambient conditions and elevated temperatures. However, the current major limitations of existing electrides include their poor thermal stability and inefficient control over the concentration of the electron anions. Two major classes of electrides were developed. Complexes of alkali metal atoms and organic molecules, such as cryptands and crown ethers, form organic electrides.[3−6] The interaction between the molecules and alkali atoms favors effective ionization of the latter and formation of a positively charged framework built of the molecules and positive alkali ions. The framework charge is compensated by the electron anions localized in the cavities between the molecules. The first thermally stable organic electride has been synthesized only very recently.[7] Zeolites heavily doped with alkali atoms represent an example of inorganic electrides.[8−16] For example, Cs atoms incorporated into zeolite ITQ-4 form ordered zigzag chains of Cs^+ ions.[15] Their charge is compensated by electron anions also distributed in a chain parallel to that of Cs^+.[17] Such electronic structure and the ordered distribution of the electron anions in electrides are not found in, for example, *n*-doped semiconductors or systems containing solvated electrons.[18,19]

In this work, we consider a complex oxide $12CaO \cdot 7Al_2O_3$ (C12A7) that can be converted from an insulator to a novel electride. C12A7 electride is stable at room temperature, has a work function of only 0.6 eV, and exhibits properties promising

† University College London.
‡ Japan Science and Technology Agency, Tokyo Institute of Technology.
§ Frontier Collaborative Research Center and Materials and Structures Laboratory, Tokyo Institute of Technology.

(1) Dye, J. L. *Science* **2003**, *301*, 607−608.
(2) Dye, J. L. *Science* **1990**, *247*, 663−668.
(3) Dye, J. L. *Prog. Inorg. Chem.* **1984**, *32*, 327−441.
(4) Dye, J. L.; Debacker, M. G. *Annu. Rev. Phys. Chem.* **1987**, *38*, 271−301.
(5) Wagner, M. J.; Dye, J. L. *Annu. Rev. Mater. Sci.* **1993**, *23*, 223−253.
(6) Dye, J. L. *Inorg. Chem.* **1997**, *36*, 3816−3826.
(7) Redko, M. Y.; Jackson, J. E.; Huang, R. H.; Dye, J. L. *J. Am. Chem. Soc.* **2005**, *127*, 12416−12422.
(8) Barrer, R. M.; Cole, J. F. *J. Phys. Chem. Solids* **1968**, *29*, 1755−1758.
(9) Srdanov, V. I.; Haug, K.; Metiu, H.; Stucky, G. D. *J. Phys. Chem.* **1992**, *96*, 9039−9043.
(10) Blake, N. P.; Metiu, H. *J. Chem. Phys.* **1998**, *109*, 9977−9986.
(11) Sankey, O. F.; Demkov, A. A.; Lenosky, T. *Phys. Rev. B* **1998**, *57*, 15129−15139.
(12) Srdanov, V. I.; Stucky, G. D.; Lippmaa, E.; Engelhardt, G. *Phys. Rev. Lett.* **1998**, *80*, 2449−2452.
(13) Madsen, G. K. H.; Gatti, C.; Iversen, B. B.; Damjanovic, L.; Stucky, G. D.; Srdanov, V. I. *Phys. Rev. B* **1999**, *59*, 12359−12369.
(14) Lushchik, C.; Demidenko, V.; Kirm, M.; Kudryavtseva, I.; Lushchik, A.; Martinson, I.; Nagirnyi, V.; Vasil'chenko, E. *J. Phys.: Condens. Matter* **2001**, *13*, 6133−6149.
(15) Petkov, V.; Billinge, S. J. L.; Vogt, T.; Ichimura, A. S.; Dye, J. L. *Phys. Rev. Lett.* **2002**, *89*, 075502.
(16) Ichimura, A. S.; Dye, J. L.; Camblor, M. A.; Villaescusa, L. A. *J. Am. Chem. Soc.* **2002**, *124*, 1170−1171.
(17) Li, Z.; Yang, J.; Hou, J. G.; Zhu, Q. *J. Am. Chem. Soc.* **2003**, *125*, 6050−6051.
(18) Liu, X.; Zhang, G.; Thomas, J. K. *J. Phys. Chem. B* **1997**, *101*, 2182−2194.
(19) Gutowski, M.; Hall, C. S.; Adamowicz, L.; Hendricks, J. H.; de Clercq, H. L.; Lyapustina, S. A.; Nilles, J. M.; Xu, S.-J.; Bowen, K. H., Jr. *Phys. Rev. Lett.* **2002**, *88*, 143001.

 10.1021/ja066177w CCC: $37.00

for applications in chemistry, electronic devices, and other areas.[21,23−26] We use ab initio calculations to develop a consistent model of this system at different concentrations of the electron anions.

The unusual properties of C12A7 originate from its crystalline structure: it consists of a positively charged lattice framework, which is compensated by negative extraframework species. The stoichiometric cubic unit cell has the size of[20] 11.99 Å and is represented by the formula $[Ca_{24}Al_{28}O_{64}]^{4+}\cdot 2O^{2-}$, where the first part denotes the framework built of 12 cages, whereas the O^{2-} ions are extraframework species that occupy two out of 12 framework cages. It has recently been experimentally demonstrated that C12A7 can be reduced so that part or all of its extraframework O^{2-} ions are replaced with an equivalent number of extraframework electrons, the concentration of which, n_e, can reach $\sim 2 \times 10^{21}$ cm^{-3}.[21] As we show below, these electrons occupy the former O^{2-} ion sites and play the role of anions. The experimental results demonstrate that as the value of n_e increases, C12A7 transforms from an insulator to a polaron conductor and then to a metal.[21,22] Mechanisms involved in these processes are not yet fully understood.

We note that the formation of the extraframework electrons in C12A7 does not require the incorporation of alkali atoms. Instead, they can be formed via several procedures (some of which are mentioned below), and their concentration in the same sample can be varied reversibly.[24] These properties of C12A7 make it different from other electrides. As we have noted previously,[27] this also offers an interesting possibility for studying the properties of confined three-dimensional electron gas in a wide range of concentrations.

However, accurately modeling the properties of systems where the concentration of electrons forming the electron gas can vary by several orders of magnitude represents a formidable challenge. Most of the ab initio methods used in practical applications are suited to deal with either insulating or metallic systems. For example, it is well documented that the Hartree−Fock (HF) based methods tend to overlocalize the electron density and overestimate the band gap by as much as 60−100% (see, for example, refs 28 and 29 and references therein). The HF approach can reproduce main characteristics of insulators, but it is not well suited for studying metallic systems. On the other hand, most of the methods based on the density functional theory (DFT) tend to overdelocalize the electron density and underestimate the band gap by as much as 50%. Moreover, in some cases, DFT offers metallic solutions for insulators and semiconductors. The situation can be improved by using, for example, hybrid density functionals, which contain the exact exchange contribution[30,31] and more sophisticated methods effectively eliminating self-interaction.[32−34] Yet there is little evidence that these methods are able to reproduce the insulator−metal transition accurately.

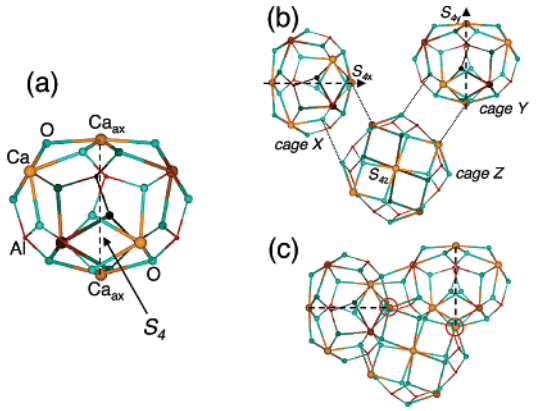

Figure 1. Structure of the C12A7 framework: (a) a single cage, (b) three neighboring cages (X, Y, and Z) with differently oriented S_4 symmetry axes S_{4x}, S_{4y}, and S_{4z}, respectively (S_{4z} is perpendicular to the plane of the figure), (c) the same three cages connected together. Dashed lines indicate the S_4 axes and corresponding directions. Axial Ca$_{ax}$ atoms are explicitly indicated in (a). Thin dotted lines in (b) connect atoms that occupy the same lattice sites. Cages X and Y are nearest neighbors to cage Z and next nearest neighbors to each other.

In this article, we report the geometric structure and electron density distribution of C12A7 calculated using a periodic model, two density functionals, and a localized basis set. The two selected density functionals are widely used in studies of insulators and metals, respectively, and each is expected to describe accurately at least one of the limits of n_e. Through a consistent set of calculations, we demonstrate that in the limit of small n_e the electron anions induce a strong lattice relaxation and become well localized; their properties resemble the properties of color centers in insulators. In the limit of large n_e, the electron anions can be considered as a weakly inhomogeneous low-density electron gas confined within the inert host lattice. Surprisingly, even in this case the charge density distribution retains a partially localized character.

2. Experimental and Theoretical Background

2.1. Structure of C12A7. As mentioned above, C12A7 can be viewed as a network of positively charged cages populated by O^{2-} extraframework species that occupy two out of 12 framework cages. The framework contains $\sim 7 \times 10^{21}$ ellipsoid-like cages/cm^3 each having ~4 Å of free inner space. Each cage (Figure 1a) is composed of six Ca, eight Al, and 16 O ions. All Ca atoms of the framework are equivalent; however, they occupy different lattice sites with respect to the cage center. More specifically, two Ca ions that occupy the sites on the opposite sides of the cage (cage poles) define an S_4 symmetry axis passing through the cage center and will be referred to as *axial* Ca atoms or Ca$_{ax}$.

The 12 cages of the cubic unit cell are equivalent and form three groups of four cages each with their S_4 symmetry axes directed along *x*, *y*, and *z* crystallographic axes and denoted as S_{4x}, S_{4y}, and S_{4z}, respectively (Figure 1b). Each group of four cages is divided further

(20) Bartl, H.; Scheller, T. *Neues Jahrb. Mineral. Monatsh.* **1970**, *35*, 547−552.
(21) Matsuishi, S.; Toda, Y.; Miyakawa, M.; Hayashi, K.; Kamiya, T.; Hirano, M.; Tanaka, I.; Hosono, H. *Science* **2003**, *301*, 626−629.
(22) Kim, S. W.; Matsuishi, S.; Nomura, T.; Kubota, Y.; Takata, M.; Hayashi, K.; Kamiya, T.; Hirano, M.; Hosono, H. Unpublished data, 2006.
(23) Hayashi, K.; Hirano, M.; Matsuishi, S.; Hosono, H. *J. Am. Chem. Soc.* **2002**, *124*, 738−739.
(24) Hayashi, K.; Matsuishi, S.; Kamiya, T.; Hirano, M.; Hosono, H. *Nature* **2002**, *419*, 462−465.
(25) Toda, Y.; Matsuishi, S.; Hayashi, K.; Ueda, K.; Kamiya, T.; Hirano, M.; Hosono, H. *Adv. Mater.* **2004**, *16*, 685−689.
(26) Matsuishi, S.; Hayashi, K.; Hirano, M.; Hosono, H. *J. Am. Chem. Soc.* **2005**, *127*, 12454.
(27) Sushko, P. V.; Shluger, A. L.; Hayashi, K.; Hirano, M.; Hosono, H. *Phys. Rev. Lett.* **2003**, *91*, 126401.
(28) Corá, F.; Alfredsson, M.; Mallia, G.; Middlemiss, D. S.; Mackrodt, W. C.; Dovesi, R.; Orlando, R. *Struct. Bonding* **2004**, *113*, 171−232.
(29) Bylander, D. M.; Kleinman, L. *Phys. Rev. B* **1990**, *41*, 7868−7871.
(30) Becke, A. D. *J. Chem. Phys.* **1993**, *98*, 5648−5652.
(31) Muscat, J.; Wander, A.; Harrison, N. M. *Chem. Phys. Lett.* **2001**, *342*, 397−401.
(32) Kralik, B.; Chang, E. K.; Louie, S. G. *Phys. Rev. B* **1998**, *57*, 7027−7036.
(33) Robertson, J.; Xiong, K.; Clark, S. J. *Thin Solid Films* **2006**, *496*, 1−7.
(34) Vydrov, O. A.; Scuseria, G. E.; Perdew, J. P.; Ruzsinszky, A.; Csonka, G. I. *J. Chem. Phys.* **2006**, *124*, 094108.

into two subgroups of two cages that have different chirality and denoted using + and − signs (e.g., S_{4z+} and S_{4z-}). The cages of the same chirality form a body-centered cubic (bcc) lattice with the distance between the cage centers of about 10 Å.

Each cage is connected to eight nearest neighbor (*nn*) cages and to four next nearest neighbor (*nnn*) cages. For example, cages S_{4x} and S_{4y} in Figure 1b are *nn* cages to S_{4z} and *nnn* cages to each other. The openings between *nn* cages have a relatively large area, with the distance between the opposite sides of each opening close to 3.7 Å, which may allow for in- and out-diffusion of atoms, ions, and small molecules.

Thus, the whole framework can be represented as six interlocked bcc lattices of interconnected cages, which can be considered as positively charged vacancies with the charge of +1/3 |e| per cage. As we discuss below, this has a dramatic effect on the electronic structure of this material.

A wide variety of negatively charged extraframework species can be incorporated into C12A7 to compensate for the positive charge of the framework ($\sim 2.3 \times 10^{21}$ $|e|/cm^3$). We emphasize that the extraframework species are necessarily present in C12A7 and should be considered not as defects but rather as a disordered component of the lattice, where the disorder applies to both their chemical identity and spatial distribution. The chemical identity and relative concentrations of the extraframework species can be controlled by an appropriate choice of the preparation conditions. It has been demonstrated that the O^{2-} ions can be partially or fully replaced with other extraframework species including, for example, OH^-,[35,36] O^{2-},[37,38] O^-,[23,39] H^-,[24] and electrons.[21] In this article, we will use C12A7:e^- to define C12A7 containing extraframework electrons. The system with the maximum concentration of four extraframework electrons per cubic unit cell will be called C12A7:$(e^-)_4$ or C12A7 electride.

2.2. Experimental Data. In this section, we briefly summarize the results of the experimental characterization of C12A7 at different concentrations of the extraframework electrons, n_e. "As grown" C12A7 is a wide band gap insulator. It is optically transparent and shows no signs of unpaired electron spin. A relatively low concentration of extraframework electrons in C12A7 ($n_e \approx 10^{19}$ cm^{-3}) can be generated by UV irradiation of H-doped C12A7.[24,40,41] The formation of the extraframework electrons is manifested by the appearance of the unpaired electron spin, detected via electron paramagnetic resonance (EPR) spectroscopy and thermally activated electrical conductivity. In addition, two optical absorption bands appear with maxima at 0.4 and 2.8 eV. Formation of electron anions in this material can be also induced via bombardment of H-doped C12A7 with electrons[42] and ions.[43] In addition, the electride phase can be formed directly from C12A7 melt.[44]

The transition from the low to high values of n_e has been investigated using an additive coloration technique and different exposure times of "as grown" C12A7 to the metal Ca vapor.[21] The optical and electrical properties of the material change significantly as n_e is increased from zero to $\sim 2 \times 10^{21}$ cm^{-3}, which corresponds to approximately the maximum concentration of four e^- per cubic unit cell.

First, the absolute intensities of the optical absorption bands at 2.8 and 0.4 eV increase dramatically, and their relative intensities change from $I_{2.8}/I_{0.4} = 1/6$ at low n_e ($\sim 10^{19}$ cm^{-3}) to about $I_{2.8}/I_{0.4} = 1/3$ at high n_e.

Second, the measurements of the temperature dependence of the electrical conductivity suggest that the conductivity activation energy decreases with increasing n_e. Importantly, even at the highest obtained concentrations the electrical conductivity remained thermally activated.[21] However, the results of recent experiments carried out on better prepared C12A7 samples treated with metal Ti suggest that the electrical conductivity changes its nature with the concentration and acquires metallic character at concentrations higher than 10^{21} cm^{-3}.[22]

Finally, it has been found that the concentration of unpaired electron spins does not follow the total number of extraframework electrons. Instead, it reaches a saturation at 5×10^{19} cm^{-3}, and therefore the system adopts such a spin state where most of the extraframework electrons, localized in neighboring cages, couple their spins antiferromagnetically. The remaining unpaired electron spins are distributed randomly and form a spin glass at low temperatures.[21]

2.3. Theoretical Models. The electronic structure calculations of C12A7 in the limit of dilute extraframework electrons (small n_e) were first carried out using an embedded cluster approach and B3LYP density functional.[27,41,45] It has been concluded that C12A7 has two conduction bands: the upper conduction band is due to cation states of the framework, framework conduction band (FCB), whereas the lower, more narrow conduction band is formed by the states associated with the cages, cage conduction band (CCB). (The charge density of CCB states calculated in this work is shown in section 5.) We have found that the states of the CCB are not associated with any particular framework ions since the empty space of each cage is much larger than the framework interatomic distances. Instead, they can be viewed as linear combinations of 1s-like states of a particle in a "box", where the "boxes" are formed by the walls of the framework cages (section 5).

When electrons substitute the extraframework anions, they occupy some of the CCB states and induce a strong lattice relaxation, which further facilitates the electron localization in cages (i.e., formation of polarons). The optical absorption band at 0.4 eV was assigned to the cage-to-cage charge-transfer excitations, and the band at 2.8 eV was assigned to intracage transitions from an s-like state of the localized electron to the p-like states split from the bottom of the FCB and associated with the same cage.[27,45] The calculated activation energy for the thermally activated electron hopping was found to be 0.1−0.2 eV and is consistent with the experimentally obtained value of 0.1 eV.[24]

An alternative model for the properties of extraframework electrons in C12A7 has been put forward on the basis of the DFT calculations performed using a linear muffin-tin orbital method.[46,47] It has been suggested that in H-doped C12A7 the extraframework electrons hop along the pathways formed by framework Ca atoms and extraframework H atoms and OH^- ions, but not by the empty cages. It has been suggested that C12A7 can exhibit "bulk conductivity" if electrons are the only extraframework species. In this case, the extraframework electrons are not localized in the cages but distributed over the lattice, while cages contribute on average 2.6% to the DOS in the vicinity of the Fermi energy. These electrons occupy a hybrid sub-band at the bottom of the conduction band.[47] For completeness, we mention that the position of this sub-band is qualitatively similar to the position of

(35) Imlach, J. A.; Glasser, L. S. D.; Glasser, F. P. *Cem. Concr. Res.* **1971**, *1*, 57−61.
(36) Li, J.; Huang, F.; Wang, L.; Yu, S. Q.; Torimoto, Y.; Sadakata, M.; Li, Q. X. *Chem. Mater.* **2005**, *17*, 2771−2774.
(37) Hosono, H.; Abe, Y. *Inorg. Chem.* **1987**, *26*, 1192−1195.
(38) Matsuishi, S.; Hayashi, K.; Hirano, M.; Tanaka, I.; Hosono, H. *J. Phys. Chem. B* **2004**, *108*, 18557−18568.
(39) Hayashi, K.; Matsuishi, S.; Hirano, M.; Hosono, H. *J. Phys. Chem. B* **2004**, *108*, 8920−8925.
(40) Sushko, P. V.; Shluger, A. L.; Hayashi, K.; Hirano, M.; Hosono, H. *Appl. Phys. Lett.* **2005**, *86*, 092101.
(41) Sushko, P. V.; Shluger, A. L.; Hayashi, K.; Hirano, M.; Hosono, H. *Phys. Rev. B* **2006**, *73*, 045120.
(42) Hayashi, K.; Toda, Y.; Kamiya, T.; Hirano, M.; Yamanaka, M.; Tanaka, I.; Yamamoto, T.; Hosono, H. *Appl. Phys. Lett.* **2005**, *86*, 022109.
(43) Miyakawa, M.; Hayashi, K.; Hirano, M.; Toda, Y.; Kamiya, T.; Hosono, H. *Adv. Mater.* **2003**, *15*, 1100−1103.
(44) Kim, S. W.; Miyakawa, M.; Hayashi, K.; Sakai, T.; Hirano, M.; Hosono, H. *J. Am. Chem. Soc.* **2005**, *127*, 1370−1371.
(45) Sushko, P. V.; Shluger, A. L.; Hayashi, K.; Hirano, M.; Hosono, H. *Thin Solid Films* **2003**, *445*, 161−167.
(46) Medvedeva, J. E.; Freeman, A. J.; Bertoni, M. I.; Mason, T. O. *Phys. Rev. Lett.* **2004**, *93*, 016408.
(47) Medvedeva, J. E.; Freeman, A. J. *Appl. Phys. Lett.* **2004**, *85*, 955−957.

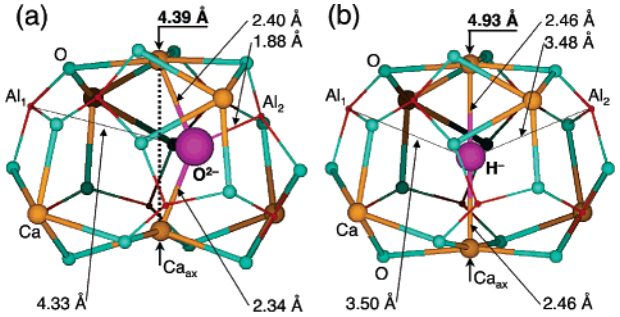

Figure 2. Local atomic structure of extraframework species in C12A7 calculated using periodic model and B3LYP density functional: (a) a cage containing an extraframework O^{2-} ion, (b) a cage containing an extraframework H^- ion. The distance between the Ca_{ax} ions at the cage poles (D_{S4}) is shown in both cases. A pair of Al ions, which are equivalent in an undistorted cage, is shown as Al_1 and Al_2. Bonding between the extraframework O^{2-} and Al_2 in (a) results in a significant deformation of the cage wall. The dotted line in (a) shows the S_4 symmetry axis of an undistorted cage.

the cage conduction band in our calculations although its nature and the magnitude of splitting from the framework conduction band are different.

A different model for C12A7 with the maximum concentration of the extraframework electrons (C12A7 electride) was suggested on the basis of periodic plane-wave DFT calculations.[48] The band structure of C12A7 electride reported there clearly shows a narrow partially occupied band. The extraframework electrons that fill this band are, according to the density integration analysis, delocalized equally over 12 cages of the cubic unit cell so that the corresponding chemical formula can be written as $[Ca_{24}Al_{28}O_{64}]^{4+}\cdot(1/3\ e^-)_{12}$. We note that the band structure reported in Figure 2 of ref 48 shows two different sets of one-electron energies for the Γ point, which may suggest that an erroneous selection of k points was taken for the analysis of the results.

Thus, two mutually excluding models for the electronic structure and spatial localization of the extraframework electrons in C12A7 electride have been reported. In this work, we present a systematic study of the C12A7 electronic structure for different concentrations of the extraframework electrons using the periodic model and two types of density functionals. In all cases, we use the same computational scheme and the same basis set, which allows us to make direct comparison of several computational methods and elucidate further the properties of this complex system.

3. Details of the Calculations

The C12A7 structure was modeled using a cubic unit cell with 116-atom framework $[Ca_{24}Al_{28}O_{64}]^{4+}$ and several combinations of negatively charged extraframework species. For convenience, we use the lattice spacing of 12.0 Å, which is close to the experimental value of 11.99 Å.[20] First, we study an insulating C12A7 where two types of the extraframework species were considered: (i) "as grown" C12A7 containing two extraframework O^{2-} ions and (ii) C12A7 containing four extraframework H^- ions, which can be obtained experimentally under aggressive chemical treatment. Then we investigate the properties of the extraframework electrons in C12A7. For that, H^- ions are gradually replaced by electrons and changes of the lattice geometry and electronic structure as a function of electron concentration are monitored.

The calculations were performed using the CRYSTAL-03 code[49] in which Bloch functions are expanded over linear combination of localized atom-centered Gaussian-type basis functions. Such methods (generally known as LCAO for linear combination of atomic orbitals) are routinely used to describe properties of insulators and semiconductors.[28,50,51] The applicability of LCAO basis to studying metals has been explored only relatively recently (see, for example, refs 52−55).

One of the advantages of the Gaussian-type basis is the possibility to use efficiently both Hartree−Fock and DFT methods within one computational scheme. As we mentioned in the Introduction, it is hard to expect that both insulating and metallic states of C12A7 could be reproduced equally accurately within one computational approach. Here, we used two density functionals based on the local density approximation (LDA) and generalized gradient approximation (GGA), respectively. The LDA functional combines Dirac−Slater exchange[56] with Vosko−Wilk−Nusair parametrization of the free electron gas correlation.[57] This functional is often used in the studies of metals. The hybrid B3LYP density functional, which is a widely used variant of a GGA functional, was also employed in this work. It combines Becke's exchange functional[30] with the correlation functional by Lee, Yang, and Parr.[58] The exchange part of the B3LYP functional contains a 20% contribution of the exact exchange, which proved to be essential for accurate modeling of polaron states in insulators.[59−61] Although the exchange part of the B3LYP functional was fitted to reproduce the properties of atoms and small molecules, it has been well documented that this functional also reproduces band gaps of insulators and wide band gap semiconductors,[31] which is important for success of this work.

Effective core pseudopotentials (ECP) were used to represent Ca, Al, and O atoms so that their electronic configurations were $[1s^22s^22p^6]3s^23p^64s^2$ for Ca, $[1s^22s^22p^6]3s^23p^1$ for Al, and $[1s^2]2s^22p^4$ for O atoms, where square brackets show the core electrons represented using ECPs. For Ca atoms, we used "small core" ECP by Hay and Wadt[62] and (3s3p1d) basis set; Al and O atoms were represented using ECP by Durand and Barthelat[63] and (2s2p1d) and (2s2p) basis sets, respectively. Double-ζ basis set cc-pVDZ[64] was used for H atom. Finally, a set of three sp shells was positioned at the center of each cage unoccupied by extraframework atoms. The exponential factors α for these functions were evenly scaled via $\alpha_{i+1} = k^i\alpha_1$, where $k = 0.46$ and $\alpha_1 = 1.022$ Bohr^{-2}. Such an extension of the atom-centered basis set was necessary to make sure that extraframework electrons have enough variational freedom to accommodate themselves everywhere in the lattice.

Since the C12A7 unit cell is large, most of the calculations were carried out using the Γ point only. However, the dependence of the results on the choice of the Monkhorst−Pack mesh has been investigated for C12A7 electride.

4. Results of the Calculations

4.1. Insulating C12A7. To model "as grown" C12A7, we positioned two extraframework O^{2-} ions in two S_{4z+} cages, that is, their sublattice forms a bcc lattice (section 2.1) with the smallest distance between the centers of the occupied cages of

(48) Li, Z.; Yang, J.; Hou, J. G.; Zhu, Q. *Angew. Chem., Int. Ed.* **2004**, *43*, 6479−6482.
(49) Saunders, V. R.; Dovesi, R.; Roetti, C.; Orlando, R.; Zicovich-Wilson, C. M.; Harrison, N. M.; Doll, K.; Civalleri, B.; Bush, I. J.; D'Arco, Ph.; Llunell, M. *CRYSTAL2003 User's Manual*; University of Torino: Torino, Italy, 2003.
(50) Hehre, W. J.; Radom, L.; Schleyer, P. V. R.; Pople, J. A. *AB INITIO Molecular Orbital Theory*; Wiley & Sons: New York, 1986.
(51) Causá, M.; Dovesi, R.; Roetti, C. *Phys. Rev. B* **1991**, *43*, 11937−11943.
(52) Boettger, J. C.; Trickey, S. B. *Phys. Rev. B* **1995**, *51*, 15623.
(53) Jaffe, J. E.; Lin, Z.; Hess, A. C. *Phys. Rev. B* **1998**, *57*, 11834−11837.
(54) Doll, K.; Harrison, N. M. *Phys. Rev. B* **2001**, *63*, 165410.
(55) de Bas, B. S.; Dorsett, H. E.; Ford, M. J. *J. Phys. Chem. Solids* **2003**, *64*, 495−505.
(56) Dirac, P. A. M. *Proc. Cambridge Philos. Soc.* **1930**, *26*, 376.
(57) Vosko, S. H.; Wilk, L.; Nusair, M. *Can. J. Phys.* **1980**, *58*, 1200−1211.
(58) Lee, C.; Yang, W.; Parr, R. G. *Phys. Rev. B* **1988**, *37*, 785−789.
(59) Pacchioni, G.; Frigoli, F.; Ricci, D.; Weil, J. A. *Phys. Rev. B* **2001**, *63*, 054102.
(60) Laegsgaard, J.; Stokbro, K. *Phys. Rev. Lett.* **2001**, *86*, 2834−2837.
(61) Gavartin, J. L.; Sushko, P. V.; Shluger, A. L. *Phys. Rev. B* **2003**, *67*, 035108.
(62) Hay, P. J.; Wadt, W. R. *J. Chem. Phys.* **1985**, *82*, 299−310.
(63) Durand, P.; Barthelat, J. C. *Theor. Chim. Acta* **1975**, *38*, 283−302.
(64) Kendall, R. A.; Dunning, T. H.; Harrison, R. J. *J. Chem. Phys.* **1992**, *96*, 6796−6806.

Table 1. Geometrical Parameters of C12A7 Cages Calculated for Different Chemical Compositions of the Extraframework[a]

density functional	extraframework	Ca_{ax}–Ca_{ax} distance (D_{S4}), Å			
		empty	O^{2-}	H^-	e^-
B3LYP	$2O^{2-}$	5.64	4.39		
	$4H^-$	5.63		4.93	
	$3H^-$ $1e^-$	5.62		4.95	5.06
	$2H^-$ $2e^-$	5.62		4.96	5.09
	$1H^-$ $3e^-$	5.63		4.99	5.10
	$4e^-$	5.63			5.13
LDA	$3H^-$ $1e^-$	5.65		4.98	5.13
	$2H^-$ $2e^-$	5.68		5.07	5.33
	$1H^-$ $3e^-$	5.68		5.12	5.38
	$4e^-$	5.69			5.41

[a] The average distances between the Ca_{ax} atoms at the cage poles (D_{S4}) are shown for unoccupied (empty) cages as well as for those occupied by extraframework O^{2-} and H^- ions and e^-. The data are given for the electronic states with maximum total spin. The charge density was calculated using the Γ point only.

about 10 Å. The total energy of the system has been fully minimized with respect to the fractional coordinates of the unit cell.

Figure 2a shows the local atomic configuration of an extraframework O^{2-} in a C12A7 cage. It is clear that the cage wall is strongly distorted as both Ca_{ax} ions and one Al ion (shown as Al_2 in Figure 2a) displace approximately toward the cage center. At the same time, the extraframework O^{2-} ion moves closer to Al_2 into an off-center site and becomes effectively three-coordinated. To highlight the extent of the cage distortion, we indicated the site Al_1, which is equivalent to Al_2 in an empty cage.

The lattice distortion is driven by the formation of strong ionic bonds between the three cage wall cations (Ca_{ax} and Al_2) and the extraframework O^{2-} ion. We also found a metastable on-center configuration of the extraframework O^{2-}, in which the central O^{2-} is coordinated by two Ca_{ax} ions only. The energy of this on-center configuration is higher than that of the off-center one by 0.2 eV.

The distance between two Ca_{ax} atoms at the poles of a cage (D_{S4}) is a convenient parameter to quantify the magnitude of the cage wall distortion. We found that in the cages occupied by O^{2-} ions $D_{S4} = 4.39$ Å, whereas in the empty cages $D_{S4} = 5.66$ Å. Such changes in the values of D_{S4} distances are a general feature of the lattice relaxation induced by negative extraframework species in this material (Table 1). The distances between the extraframework O^{2-} and two Ca_{ax} ions and Al_2 ion are 2.40, 2.34, and 1.88 Å, respectively. We note that these values are close to those obtained by us earlier using an embedded cluster approach: 2.46, 2.41, and 2.18 Å, respectively.[65] Thus, both periodic and embedded cluster schemes give a very similar local atomic structure. The difference of 0.3 Å in the bond lengths of the extraframework O^{2-} with Al_2 does not affect the electronic structure of this system.

The band structure calculated for stoichiometric C12A7 is shown in Figure 3a. The states below −5.0 eV form the valence band (VB) composed of 2p states of the framework O^{2-} ions. The strong lattice relaxation induced by the extraframework O^{2-} ions splits several framework O 2p states from the top of the VB. These, as well as 2p states of the extraframework O^{2-}, occupy a broad energy region between −5.0 and −3.0 eV and effectively narrow down the apparent band gap of stoichiometric C12A7.[66] The almost zero dispersion found for these states shows that they are well localized. We note that, in the case of a metastable on-center configuration, the distortion of the cage wall is much smaller, and consequently, no 2p states associated with the framework oxygens appear in the band gap.

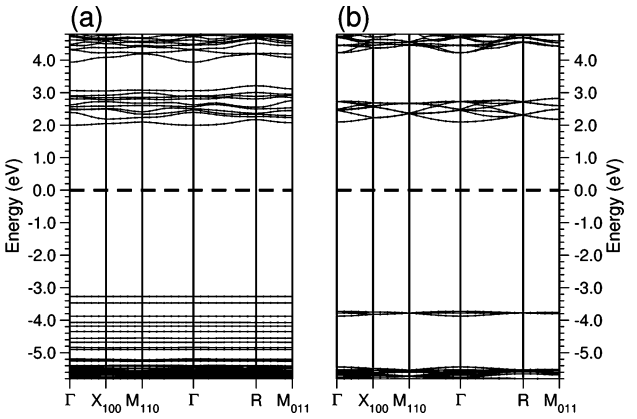

Figure 3. Band structure of insulating C12A7 calculated using B3LYP for two chemical compositions of the extraframework containing: (a) two O^{2-} and (b) four H^- ions. Thick dashed line indicates the position of the Fermi energy. The bands are plotted along the lines connecting *k* points Γ (0,0,0), X(1,0,0), M(1,1,0), Γ (0,0,0), R(1,1,1), and M(0,1,1). Note that points M(1,1,0) and M(0,1,1) in (b) are not equivalent due to the lattice distortion induced by the extraframework ions.

The states above 2.0 eV (Figure 3a) are unoccupied and form two bands. The lower band at 2.0−2.8 eV consists of 10 states associated with 10 unoccupied cages (cage conduction band), while the states at 4.2 eV and above are associated with the framework (framework conduction band).

To model C12A7 containing four H^- ions per unit cell, these ions were positioned in four S_z cages (two S_{4z+} and two S_{4z-} cages) forming two interlocked bcc lattices. The local atomic structure for an extraframework H^- ion incorporated in a C12A7 cage is shown in Figure 2b. It is clear that H^- ions also induce a noticeable lattice distortion due to the interaction with the positively charged cage wall, although the overall displacement of atoms is much smaller than that in the case of O^{2-}. We note that the corresponding $D_{S4} = 4.93$ Å is about 0.5 Å closer to its value in the empty cage than in the case of extraframework O^{2-} (see also Table 1). This further emphasizes the fact that the smaller the charge of an extraframework species, the smaller the lattice distortion it induces.

The band structure of H^- containing C12A7 is shown in Figure 3b. We will only indicate the differences with respect to the case of the extraframework O^{2-} ions. (i) The six energy levels of extraframework O^{2-} ions are replaced by four levels due to H^- ions at about 1.6 eV above the top of the VB. These states show a nonzero dispersion, yet our analysis suggests that they are well localized within the four cages occupied by H^-. (ii) The smaller charge of H^- ions and the lattice relaxation they induce provide a local perturbation that is not sufficient to split framework O 2p states from the top of the VB. (iii) The CCB becomes slightly narrower since it now contains only eight states per unit cell.

(65) Sushko, P. V.; Shluger, A. L.; Hayashi, K.; Hirano, M.; Hosono, H. *Phys. Rev. B* **2006**, *73*, 014101.

(66) Hayashi, K.; Sushko, P. V.; Muñoz Ramo, D.; Shluger, A. L.; Watauchi, S.; Tanaka, I.; Matsuishi, S.; Hirano, M.; Hosono, H. *J. Phys. Chem. B*, in press.

Interestingly, the local geometry of the unoccupied cages, as characterized by the corresponding D_{S4} distances, remains almost unaffected when one type of extraframework species is replaced by another. For example, D_{S4} increases by nearly 0.5 Å when O^{2-} is replaced by H^- and D_{S4} decreases by about the same 0.5 Å when an extraframework electron is introduced into a previously unoccupied cage. Yet, the D_{S4} in the unoccupied cages varies by no more than 0.02 Å (Table 1). This is explained by the relative orientation and the structure of the cages: (i) the S_4 symmetry axes of the neighboring cages are perpendicular to each other and (ii) Ca_{ax} atoms at the poles of each cage belong to cage walls (but not poles) of the neighboring cages. Thus, the deformations of the cages along S_4 axes are almost uncoupled from each other.

Finally, we analyze the charge density distribution of C12A7 using Mulliken population analysis. The C12A7 framework contains one type of Ca ions, two types of Al, and two types of O atoms. In the case of H^- extraframework, there is a small difference in the atomic charges of Ca_{ax} at the poles of occupied and unoccupied cages: 1.95 and 1.94 |e|, respectively. The atomic charges of the two Al types are 1.36 and 1.29 |e|, and the charges for the two O types are −1.19 and −1.41 |e|, respectively. Finally, the charges of H^- species are close to −0.92 |e|, whereas about −0.097 |e| is associated with the basis set functions located in each unoccupied cage. The Mulliken charges of the framework atoms show little dependence on the nature of the extraframework species. Therefore, in the following section we will only discuss the charges associated with extraframework species and unoccupied cages.

4.2. C12A7:e^-: Low Electron Density Limit. The insulating C12A7 can be converted to a conductive state by extracting atomic oxygen (i.e., effectively replacing extraframework O^{2-} ions with electrons).[21] A convenient way to address theoretically the modifications of the C12A7 electronic structure at different n_e is to replace gradually the extraframework H^- ions by electrons (i.e., to consider $(H^-)_{4-n}(e^-)_n$ extraframework configurations for $n = 1, 2, 3, 4$). The effect of such a modification of the extraframework will be described in terms of the changes of the lattice geometry, electronic structure, and charge density redistribution.

First, we consider the results obtained using the B3LYP functional for the case of $n = 1$, which corresponds to the limit of low values of n_e. As an H^- ion is replaced by an electron, the corresponding cage expands and D_{S4} of that cage increases from 4.93 to 5.06 Å. All other cages are only slightly affected (Table 1).

The band structure (spin-up states only) calculated for C12A7:$(H^-)_3e^-$ is shown in Figure 4a. A new feature, as compared to the C12A7:$(H^-)_4$ band structure (Figure 3b), is the appearance of a level at 0.2 eV, which corresponds to a single extraframework electron. The dispersion of this state is comparable to that of the H^- states, which indicates that the $1s^2$ states of H^- ions and the extraframework electron state do not overlap at low n_e. This is illustrated in Figure 5, where we show the surfaces of constant charge densities associated with the H^- states, the e^- state, and the unoccupied states of the CCB. These surfaces form enclosed areas ("bubbles") positioned at the centers of the cages. Only one such "bubble" is associated with every cage.

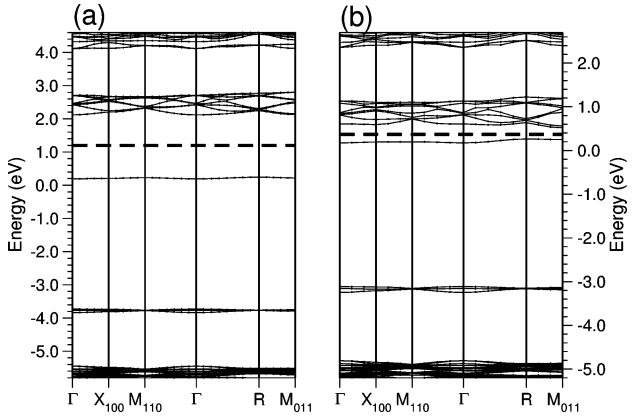

Figure 4. Band structure (spin-up states only) of C12A7:$(H^-)_3e^-$ calculated using B3LYP (a) and LDA (b) functionals. The Fermi energy is indicated with a thick dashed line. See caption to Figure 3 for notations of the k points.

Such a distribution of the charge density correlates well with the results of the Mulliken population analysis, which assigns the charge of −0.654 |e| to the cage occupied by the electron. The changes in the average Mulliken charge assigned to the unoccupied cages are negligible and amount to a slight increase from −0.097 |e| to −0.099 |e|.

Similar electronic structure and charge density distributions are obtained in LDA calculations. In this case, the one-electron state occupied by the extraframework electron is about 4.91 eV above the top of the VB and 0.46 eV below the CCB (Figure 4b). The small dispersion of this state is also very similar to that found with the B3LYP functional and, again, indicates a strongly localized state. This is further supported by the Mulliken population analysis, which assigns the charges of −0.50 |e| to a single cage occupied by an extraframework electron and −0.122 |e| to unoccupied cages, respectively. Such charge distribution, in turn, correlates with the local geometry: the calculated D_{S4} distances in the occupied and unoccupied cages are 5.13 and 5.65 Å, respectively. Thus, we conclude that both types of density functionals, B3LYP and LDA, give a similar picture of electron density distribution in C12A7:e^- at low n_e.

4.3. C12A7:$(e^-)_4$: High Electron Density Limit. As the H^- ions are gradually replaced with electrons, the B3LYP and LDA density functional give different descriptions of the electronic structure of C12A7:e^-.

In B3LYP calculations, the extraction of the first and then all consecutive H atoms has nearly exactly the same effect: average values of D_{S4} distances calculated for empty cages and for the cages occupied by the remaining H^- ions change very slightly (Table 1). The value of D_{S4} in the cages occupied by the extraframework electrons increases only marginally from 5.06 to 5.13 Å as n_e increases from one to four electrons per unit cell. The calculated energies required to extract an H atom (ΔE) also show little dependence on n_e. In particular, the values of ΔE, which can also be regarded as the formation energies of the extraframework electrons, vary between 4.33 and 4.34 eV.

As the H^- ions are gradually replaced with electrons, the narrow band due to H^- at about −3.8 eV disappears and a band due to extraframework electrons develops at 0.0−0.4 eV. The band structure calculated for C12A7:$(e^-)_4$ is shown in Figure 6a. The dispersion of this band is larger than that of the H^-

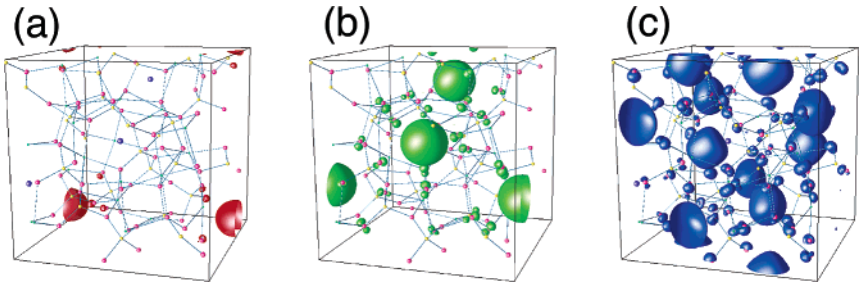

Figure 5. Surface of constant charge density calculated using B3LYP functional for the single extraframework electron (a), three H^- (b), and eight CCB (c) states. The surfaces form enclosed areas ("bubbles") positioned at the centers of the cages. Only one such "bubble" is associated with every cage. The states of the extraframework electron and CCB are not associated with any particular atom. Some of the "bubbles" are cut to show the unit cell size. The same value of the charge density was used in all three cases.

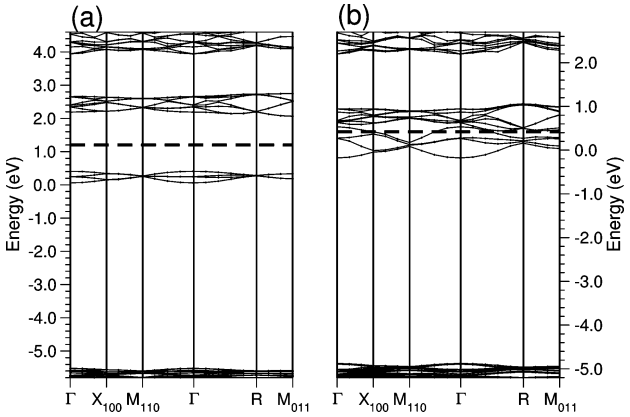

Figure 6. Band structure of C12A7:$(e^-)_4$ calculated using B3LYP (a) and LDA (b) density functionals. $3 \times 3 \times 3$ *k* mesh was used in both cases. The position of the Fermi level is shown with a thick dashed line. Only spin-up states are shown. See caption to Figure 3 for notations of *k* points.

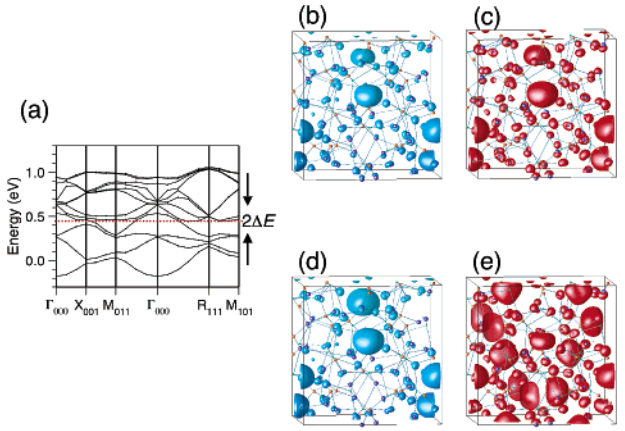

Figure 7. Electronic structure of the C12A7 electride near Fermi energy E_F. (a) Band structure of the C12A7 electride near E_F (LDA). The dashed line indicates E_F. The charge densities are calculated within ΔE below and above E_F. (b−e) Surface of constant charge density associated with the state near E_F: (b) below E_F, $\Delta E = 0.05$ eV, $\rho = 2.1 \times 10^{-3}$ e/Å^3, (c) above E_F, $\Delta E = 0.05$ eV, $\rho = 2.1 \times 10^{-3}$ e/Å^3, (d) below E_F, $\Delta E = 0.25$ eV, $\rho = 8.7 \times 10^{-3}$ e/Å^3, (e) above E_F, $\Delta E = 0.25$ eV, $\rho = 8.7 \times 10^{-3}$ e/Å^3. The states below E_F are associated with four cages only: occupied cages. The state just above the E_F ($\Delta E = 0.05$eV) is predominantly associated with the same four occupied cages. The higher states in the CCB ($\Delta E = 0.25$ eV) are associated with the empty cages.

band, pointing to a partial delocalization of these states. According to Mulliken population analysis, however, this delocalization is practically negligible and amounts to the change of the charge in the occupied cages from −0.654 to −0.645 |e| and in the empty cages from −0.099 to −0.103 |e|. Thus, even at the largest possible concentration of the extraframework electrons they remain well localized and the 12 framework cages can be clearly divided into two groups of four occupied and eight unoccupied ones.

The transition to a metallic state, observed experimentally at high n_e, is not reproduced by this approach. We attribute this to the overlocalized spatial distribution of the extraframework electrons obtained with the B3LYP functional. Indeed, we have seen earlier that the distortion of the cage wall (e.g., represented by the value of D_{S4}) is directly related to the amount of the negative charge localized within the cage. If the B3LYP density functional overestimates the localization in this case, the Ca_{ax} ions displace closer to the cage center and further contribute to the localization of the extraframework electrons.

A qualitatively different electronic structure for the limit of high n_e emerges from LDA calculations. The dispersion of the CCB states, both occupied and unoccupied, is much larger than that obtained using B3LYP. In the case of the C12A7:$(e^-)_4$ system, the gap between the four occupied and eight unoccupied states of the CCB vanishes. Close inspection of the band structure for this system (Figures 6b and 7a) suggests that the three lowest states of the CCB do not overlap with unoccupied states of the CCB in any points of the reciprocal space shown in Figure 6b. However, the fourth occupied state does: the energy of this state in the Γ point is higher than the energies of at least two unoccupied states in points X(1,0,0), M(01,1), and R(1,1,1). Thus, the C12A7:$(e^-)_4$ system should exhibit a metallic behavior.

Analysis of the atomic structure of the C12A7:$(e^-)_4$ system reveals that the lattice cages are not equivalent. Instead, they remain split into two groups of four and eight cages with D_{S4} close to 5.41 and 5.69 Å, respectively (Table 1). The Mulliken charge of −0.49 |e| is assigned to each cage with smaller D_{S4}, while only −0.13 |e| is associated with each cage with larger D_{S4}. Thus, one can still use the notion of occupied and unoccupied cages even in the case of metallic C12A7.

We investigated the dependence of the C12A7:$(e^-)_4$ system on the choice of the Monkhorst−Pack *k* mesh used in these calculations. The results obtained for different selections of *k* points are summarized in Table 2. The total energy calculated using the Γ point only (E_{1k}) differs by about 0.2 eV from that obtained using 63 *k* points (E_{63k}) selected according to $5 \times 5 \times 5$ mesh, which was a technical limit in our calculations. As the number of *k* points used in the calculations is increased, the total energy converges rapidly. For example, the difference

Table 2. Properties of C12A7:(e$^-$)$_4$ for Different Selections of Monkhorst−Pack *k* Mesh[a]

			D_{S4}		atomic charges	
k mesh	N_k	δE	empty	e$^-$	empty	e$^-$
1 × 1 × 1	1	0.000	5.695	5.375	−0.134	−0.494
2 × 2 × 2	8	−0.133	5.694	5.381	−0.160	−0.434
3 × 3 × 3	14	−0.193	5.675	5.478	−0.162	−0.427
4 × 4 × 4	36	−0.183	5.675	5.479	−0.164	−0.423
5 × 5 × 5	63	−0.186	5.679	5.492	−0.164	−0.420

[a] The relative energies δE (in eV) are calculated with respect to E_{1k} obtained using 1 × 1 × 1 mesh. Local geometries are represented using average values of D_{S4} distances (in Å) calculated for unoccupied cages (empty) and for cages occupied with electrons (e$^-$), respectively. The same applies to Mulliken atomic charges given in the units of |e|. N_k gives the total number of nonequivalent *k* points.

between E_{8k} (2 × 2 × 2 mesh) and E_{63k} is 0.05 eV, while the difference between E_{14k} (3 × 3 × 3 mesh) and E_{63k} is less than 0.007 eV.

The details of the geometry and the electronic structure of the system, as represented using the D_{S4} distances and Mulliken charges associated with the cage centers, show similar convergence trends. Both characteristics are essentially converged if the 3 × 3 × 3 *k* mesh is used, when the Mulliken charges assigned to four S_{4z} cages become −0.43 |e|, while those assigned to four S_{4x} and four S_{4y} cages become −0.16 |e|. Thus, the electronic structure of the C12A7 electride described earlier does not change in the limit of a large number of *k* points.

Finally, we investigated the magnetic properties of the C12A7:(e$^-$)$_4$ system. Starting with the atomic coordinates obtained for the state with total spin $S = 2$, we minimized the total energy for the states with the total spins $S = 1$ and $S = 0$ using the same spin-polarized B3LYP functional. The $S = 0$ state has the lowest energy, followed by $S = 1$ and $S = 2$ states, which are 0.015 and 0.028 eV higher, respectively. This is in agreement with the experimentally observed tendency of the extraframework electrons to pair their spins. The band structure and the character of the electron density distribution are the same for all three spin states. The spin pairing is even more favorable in LDA calculations, where the state with spin $S = 0$ is 0.32 eV lower than the $S = 2$ state. Such a difference between the B3LYP and LDA results is consistent with the localization of the extraframework electrons as obtained using these two functionals.

5. Discussion

5.1. Comments on the Electronic Structure of C12A7:e$^-$. Electronic structure of materials is often discussed in terms of atomic orbitals of the lattice atoms or ions. For example, the valence band of CaO is composed predominantly of 2p states of oxygen atoms, while the conduction band is formed mainly by 4s states of Ca atoms. It is tempting to apply the same type of analysis to the cage conduction band of C12A7 and to make an analogy with, for example, a narrow band of unoccupied 4f states of Ce atoms in CeO_2. However, one has to keep in mind that there is no unique method for assigning the electron density to particular atomic orbitals. Moreover, such an approach is applicable to materials where lattice atoms fill up the whole space.

A significant part of the C12A7 lattice is not occupied by atoms. Assuming that the free space inside each cage is equivalent to a sphere of the radius of 2.5 Å, about 40% of the unit cell volume is taken by the cages and cannot be associated with any lattice atoms. Another estimate, based on the ionic radii[67] of Ca^{2+} (1.00 Å), Al^{3+} (0.53 Å), and O^{2-} (1.40 Å) ions, puts the volume of the free space to as much as 50%. Thus, the electronic states of the cage conduction band can hardly be described in terms of atomic orbitals of the surrounding cage wall atoms. Instead, we suggest that a "particle in a box" description, where the "box" is formed by the cage wall, is more appropriate for this system.

The cages represent the extraframework anion sites, that is, the sites that would normally be occupied by extraframework O^{2-}, H^-, and Au^- ions compensating the positive charge of the framework. The extraframework electrons in C12A7:e$^-$ occupy the same sites as typical anions. Thus, C12A7:e$^-$ satisfies a definition of electrides.[1]

5.2. Nonmetal−Metal Transition and the Nature of State at the Fermi Level. The localized character of the extraframework electron density at low n_e agrees well with the results of our earlier embedded cluster calculations,[27,40,41,45] and it is consistent with the experimentally observed thermally activated (polaron) character of the electron conductivity.[24]

Since the extraframework electrons are not fully localized in a single cage even at low n_e, the tails of the corresponding CCB state spread out to the neighboring cages. As n_e increases, the "spill out" of the electron density from the occupied to the nominally unoccupied cages increases. This drives the relaxation of the lattice cages so that the difference between the values of D_{S4} in the cages with higher electron density and those with lower electron density decreases, which, in turn, facilitates further density distribution between the cages. The net effect of such density redistribution is that the inhomogeneity of the lattice structure induced by the extraframework species decreases and the splitting between the occupied and unoccupied CCB states decreases until it vanishes at high n_e. We note that, according to the LDA results, the extraframework electrons remain partially localized even in the metallic state (i.e., the polaron contribution to the electric conductivity can be expected at finite temperatures).

The delocalization of the extraframework electrons, correlated with the change of the lattice distortion, can be interpreted as gradual screening of the lattice localizing potential with increasing value of n_e in the spirit of nonmetal−metal (NM−M) transition discussed by Mott.[68,69] Mott criterion links the radius of the wave function of an isolated dopant a^* with its critical concentration n_c:

$$n_c^{1/3} a^* = K$$

where the value of constant $K = 0.25$ was suggested. The system becomes metallic if the concentration of the electronic centers n exceeds n_c. It has been demonstrated by Edwards and Sienko[70] that this criterion performs surprisingly well for a wide range of systems and spans 9 orders of magnitude of n_c and 600 Å of a^* if $K = 0.26 \pm 0.05$ is used. Although the electronic structure of C12A7 is more complex than the typical systems where Mott criterion is applied, in particular due to the presence of both

(67) Shannon, R. D. *Acta Crystallogr.* **1976**, 751−767.
(68) Mott, N. F. *Can. J. Phys.* **1956**, *34*, 1356−1368.
(69) Mott, N. F. *Philos. Mag.* **1961**, *6*, 287−309.
(70) Edwards, P. P.; Sienko, M. J. *J. Am. Chem. Soc.* **1981**, *103*, 2967−2971.

occupied and unoccupied CCB states and the strong polaron effect, it is instructive to see how it performs in the case of C12A7:e$^-$.

The NM−M transition in our calculations occurs at the concentrations n_e between 1.7×10^{21} and 2.3×10^{21} cm^{-3}, which corresponds to three and four extraframework electrons per unit cell, respectively. These, according to modified Mott criterion, correspond to the effective radius of an extraframework electron at low values of n_e between 2.16 and 1.97 Å, respectively. Taking D_{S4} as a measure of the cage size and considering the limit of the lowest n_e ($D_{S4} = 5.13$ Å; Table 1) and the finite diameter of the Ca ions at the cage poles (∼1.0 Å),[67] we estimate the inner diameter of the cage as 4.1 Å. This value agrees well with the effective radius of an isolated extraframework electron estimated from Mott criterion and with the localization of the extraframework electrons in cages as obtained in our calculations. We note, however, that these considerations have a qualitative character because the Mott criterion does not account for the changes of the local atomic structure, which, in our case, is a major factor behind the NM−M transition.

We considered a configuration in which the extraframework electrons occupy S_{4z} cages, while S_{4x} and S_{4y} are empty. The lattice relaxation associated with such an electronic structure makes these cages nonequivalent, which, in turn, is reflected in the band structure of C12A7:e$^-$. For example, Figure 6 shows that the one-electron energies calculated at k points M_{110} and M_{011} are different. A random distribution of the extraframework electron density over the cages is expected in a real C12A7 sample at finite temperatures. In the limit of low temperatures, a transition to a phase maximizing the distance between nominally occupied cages can be envisaged due to the repulsion between the extraframework electrons. However, the accuracy of our calculations is not sufficient to address this issue reliably.

To analyze the nature of electronic states at the Fermi level (E_F), we have calculated the charge densities due to the states in the narrow energy region ΔE near E_F as shown in Figure 7a. The surfaces of the constant charge densities below E_F ($\rho_<$) and above E_F ($\rho_>$) were calculated for $\Delta E = 0.05$ and 0.25 eV.

The $\rho_<$ due to the one-electron states below E_F are shown in Figure 7b,d and indicated by the four enclosed volumes (two of them, shown in the lower part of each plot, are split in halves due to periodic boundary conditions). Each enclosed volume is associated with an occupied cage and has a density maximum that coincides with the cage center.

Similarly, the surfaces of the constant $\rho_>$ due to the one-electron states above E_F are shown in Figure 7c,e. The $\rho_>$ in the immediate vicinity of E_F ($\Delta E = 0.05$ eV) involves the same four occupied cages, while the states due to unoccupied cages have negligible contribution to the density in this energy range (Figure 7c). However, the CCB states due to unoccupied cages dominate at higher energies (Figure 7e).

5.3. Optical Absorption of C12A7:e$^-$. One can rationalize the qualitative changes of the relative intensities of the optical absorption bands at 0.4 eV ($I_{0.4}$) and 2.8 eV ($I_{2.8}$) attributed to the cage-to-cage hopping and intracage transitions of the extraframework electrons, respectively (section 2.2). As the number of hopping electrons increases with n_e, the number of empty cages available for the intercage hopping decreases only slightly from about 10 in as grown C12A7 to eight in the C12A7 electride. Thus $I_{0.4}$ increases with n_e, although such an increase will be sublinear because the cage-to-cage motion of the electrons is not independent at high concentrations. At the same time, the intensity of the intracage transitions induced by 2.8 eV light is practically independent of the occupation of the neighboring cages, and therefore, $I_{2.8}$ is expected to increase linearly with n_e. Thus, the ratio $I_{2.8}/I_{0.4}$ should increase with n_e. These considerations apply, however, only to nonmetallic C12A7:e$^-$ where the electrons are still well localized.

We note that, although the LDA reproduces the transition of C12A7:e$^-$ to a metallic state at high n_e, it does not allow one to develop a quantitatively accurate model of the C12A7 system. For example, we compared the excitation energies of the optical transitions from the top of the valence band to the CCB states calculated using time-dependent DFT (TDDFT) and the two density functionals within the embedded cluster approach.[27] The LDA functional gives the lowest energy of only 3.9 eV, that is, significantly lower than the B3LYP result of 5.2 eV, which is more consistent with the experimental data.[66] Moreover, we could not obtain a converged TDDFT solution for the excited states of the C12A7:e$^-$ system in the case of the LDA functional.

6. Summary and Conclusions

We presented the results of the extensive set of calculations of the properties of a nanoporous oxide C12A7, which can accommodate an electron gas of different densities and be converted to an electride stable at room temperature. The unusual property of this material is that the density of the electron gas, n_e, can be changed in a controllable way in a very wide range without the loss of underlying framework structure. The value of n_e in turn affects dramatically the optical and electrical characteristics of the material. We envisage that the surface of the C12A7 electride will perform useful chemical functions, which should be possible to control by changing n_e.

To develop a consistent model of this system, we used DFT and two types of density functionals: one has a proven track record in calculations of insulators (B3LYP), while another is more suitable for metallic systems (LDA). Both functionals give the same character of the charge density distribution at low n_e: an extraframework electron is predominantly localized within a single C12A7 cage. At high values of n_e, the extraframework electrons remain highly localized in the B3LYP calculations. On the contrary, the LDA calculations show a gradual delocalization of the extraframework electrons as n_e increases. This is accompanied by a gradual decrease of the inhomogeneous lattice distortion induced by the extraframework species and by the narrowing of the gap between the occupied and unoccupied states of the CCB. The gap closes at n_e between 1.7×10^{21} and 2.3×10^{21} cm^{-3}, and the system becomes metallic. Such modifications of the C12A7:e$^-$ electronic structure are consistent with the experimental data at both low[24] and high[21,22] values of n_e. Inhomogeneous lattice distortions, which facilitate the localization of the extraframework electrons in the lattice cages, are most pronounced at low values of n_e. At high values of n_e, the extraframework electron density redistribution significantly reduces the difference in the local atomic structures of the nominally occupied and unoccupied cages.

Acknowledgment. We acknowledge fruitful discussions with S. W. Kim, S. Matsuishi, K. Hayashi, T. Kamyia, J. L. Gavartin, F. Corà, I. V. Abarenkov, and A. M. Stoneham. We thank K. McKenna for careful reading of the manuscript. This work was supported by the Grant-in-Aid for Creative Scientific Research (Grant No. 16GS0205) from the Japanese Ministry of Education, Culture, Sports, Science and Technology. The calculations were carried out on UCL Central Computing Cluster C^3 and on CSAR facility through EPSRC Grant EP/D504872.

Supporting Information Available: Parameters of the basis sets used in the calculations and supercell coordinates. This material is available free of charge via the Internet at http://pubs.acs.org.

JA066177W